

Contents lists available at ScienceDirect

Transportation Research Part B

journal homepage: www.elsevier.com/locate/trb



Maximum-stability dispatch policy for shared autonomous vehicles



Di Kang*, Michael W. Levin

Department of Civil, Environmental, and Geo- Engineering, University of Minnesota, United States

ARTICLE INFO

Article history: Received 18 July 2020 Revised 5 December 2020 Accepted 26 April 2021 Available online 12 May 2021

Keywords:
Dispatch policy
Autonomous-mobility-on-demand
Shared autonomous vehicles
Max-pressure
Stability
Maximum throughput

ABSTRACT

Shared autonomous vehicles (SAVs) have been widely studied in the recent literature. Agent-based simulations and theoretical models have extensively explored the effects on travel service, fleet size, and congestion using heuristic dispatching strategies to match SAVs with on-demand passengers. A major question that simulations have sought to address is the service rate or replacement rate: the number of passengers each SAV can serve. Thus far, the service rate has mostly been estimated through simulation. This paper investigates an analytical max-pressure dispatch policy, which aims to maximize passenger throughput under any stochastic demand pattern, which takes the form of a model predictive control algorithm. An analytical proof using Lyapunov drift techniques is presented to show that the dispatch policy achieves maximum stability. The service rate and minimum fleet sizes are derived analytically in this paper and can be achieved with the proposed dispatch policy. Simulation results show that the maximum stable demand is linearly related to the fleet size given. Also, it demonstrates how asymmetric demand necessitates rebalancing trips that affect service rates. Even though decreasing average waiting time is not the primary goal of this paper, stability ensures bounded waiting times, which is demonstrated in simulation.

© 2021 Elsevier Ltd. All rights reserved.

1. Introduction

Mobility-on-demand (MoD) services enable people to travel and share vehicles with strangers by sending the request via mobile devices. Autonomous vehicles (AVs) further promote the concept of large-scale MoD to autonomous-mobility-on-demand (AMoD) by replacing personal vehicle travel due to the lower labor costs of AV operations. AMoD advances MoD to some extent by avoiding the costs of "rebalancing drivers" to drive vehicles from over-supplied zones to under-supplied zones. Also, compared with current car-sharing companies such as Zipcar and Car2go, AMoD does not require users to return their vehicles to its origin, which provides better convenience for one-way users.

Since the cost of each AV will initially be high, shared ownership could be an economical alternative to compensate for the capital costs. Due to the lack of a driver, shared autonomous vehicles (SAVs) could provide point-to-point transportation at a price lower than operating a private AV, and also reduce the risks caused by dangerous drivers. Consequently, passengers may choose to rely on SAVs rather than owning an autonomous vehicle for daily transportation (Fagnant and Kockelman, 2015).

E-mail addresses: kang0275@umn.edu (D. Kang), mlevin@umn.edu (M.W. Levin).

^{*} Corresponding author.

From the perspective of companies who operate SAVs, they desire to maximize the passenger throughput which reduces the costs of purchasing, maintaining, and insuring a SAV fleet. Previous studies (e.g. Fagnant and Kockelman, 2014; Fagnant et al., 2015) have constructed agent-based simulations of SAV interactions with passengers on city networks and found that the replacement ratio (defined as the maximum number of conventional human-driven vehicles an SAV could replace) is between 3 and 11. Nevertheless, results are highly dependent on the passenger-to-vehicle matching policy, demand pattern, and network topology. Previous theoretical analysis on AMoD systems solving the vehicle routing problems has been focused on optimizing rebalancing vehicles (Zhang and Pavone, 2016) or based on unrealistic assumptions such as assuming no arrivals once the simulation starts (Zhang et al., 2016a). Although attempts have been made to characterize capacity-aware SAV service rates, it is not clear that the resulting dispatch policies maximize throughput (Zhang et al., 2016b). Since vehicle routing problems are in general NP-hard, studies have relied on heuristics which limit the connection between the simulation and analytical work. Although some studies have included ridesharing (one SAV serving multiple passengers simultaneously), this paper focuses on the scenario in which AVs serve one passenger at a time.

The purpose of this paper is to address the SAV dispatch problem through the notion of stability from max-pressure control of traffic signals (Varaiya, 2013). For traffic networks, stability occurs when the number of vehicles in the network remains bounded in expectation. Inefficient signal timings or sufficiently high demand prevent stability. For AMOD systems, the number of SAVs in the network is constant, but the number of waiting passengers could grow arbitrarily large if the fleet is too small to serve them. Ideally, the dispatch strategy for SAVs would maintain stability for the largest set of demands possible.

Model predictive control is used when deploying the max-pressure dispatch policy. To be more specific, the optimization program, which has the max-pressure term in the objective function, is solved for every time step. The output of optimization problems contains a series of controls for a fixed planning horizon, but only the first control actions will be executed. The remaining controls are discarded, and the optimal control for the next step will be obtained from the corresponding optimization program. Planning ahead for a fixed time horizon is used to provide vehicle relocations to serve passengers. Vehicle dispatch is re-optimized in the future to take updated traveler requests into consideration.

The contributions of this paper are as follows: (1) we formulate the SAV dispatch problem as a Markov decision process and propose a max-pressure dispatch policy; (2) we analytically characterize the set of stochastic demand that could be stabilized for any SAV systems (under the assumptions made); (3) the proposed max-pressure dispatch policy for any SAV systems is proven to serve all demand whenever possible using Lyapunov drift techniques; (4) linear programs for finding the minimum fleet size and replacement ratio are developed; and (6) a simulation model is built in Java using the IBM CPLEX API to test both off-peak and peak hour demand patterns in AMoD system in the Sioux Falls network.

The remainder of this paper is organized as follows: Section 2 discusses the previous work related to AMoD systems and how it can be integrated into the transportation network. Section 3 presents the network model and proposes a max-pressure dispatch policy. In Section 4, we prove the maximum stability property of the proposed dispatch policy. In addition, linear programs are presented to find the fleet size and replacement ratio. In Section 5, a simulation model is built to test the performance of the proposed max-pressure dispatch policy under daily and peak-hour travel demand patterns. Section 6 concludes the paper.

2. Literature review

Many previous studies of SAVs have relied on agent-based simulation. Agent-based simulations define reasonable behaviors for individual passengers and SAVs and study how they interact with each other. Many of these studies have explored the *replacement ratio*, i.e., how many passengers one SAV can serve. For example, agent-based simulations were built in Austin (a mid-sized city) (Fagnant and Kockelman, 2014), and a replacement ratio of 11 was estimated from different scenario results. Bischoff and Maciejewski (2016) tested medium and large fleet sizes of SAVs in Berlin (the largest city in Germany), and recommended replacement ratios of 10 to 12 by balancing the tradeoff between customer waiting time and vehicle's idle driving time. Martinez and Crist (2015) created a simulation model in Lisbon (capital city in Portugal) and found a replacements ratio of 10. Burns et al. (2013) examined the performance of AMoD in three different contexts: the model was run in Ann Arbor (mid-sized city), Babcock Ranch (low-density suburban city), and Manhattan (high-density urban city). Due to central coordination, SAVs implemented in Manhattan outperformed SAVs in Ann Arbor and Babcock Ranch. All of these simulations tested replacement ratios using heuristic algorithms for vehicle dispatch, so the replacement ratios they found are highly dependent on the heuristic used which makes generalization to other cities and dispatch policies difficult.

Apart from the aforementioned simulation work, analytical efforts have also been made to find a more general solution to SAV dispatch problems in previous studies. A fluid approach (Pavone et al., 2012), queuing-theoretical approach considering impatient customers (Zhang and Pavone, 2016), and Markov model (Volkov et al., 2012) were built to mathematically describe the dynamics of AMoD systems aiming to find the optimal rebalancing policy and the appropriate fleet size. However, the optimal rebalancing policy can be advanced to an optimal dispatch policy by arranging all vehicles' routes and pick-up orders rather than optimizing rebalancing trips. Braverman et al. (2019)'s recent work on re-deployment policies using a fluid model for empty vehicles provides a stochastic model to optimize utilization (availability for passengers). Instead of keeping waiting time within an acceptable range, they solve the minimum required vehicles for 100% availability. However, in reality, passengers have a certain tolerance threshold from the time they place an order to a vehicle picks this passenger

up. Taking this tolerance within the consideration, companies can run fewer vehicles than what Braverman et al. (2019) suggested. In our paper, although the waiting time is not modeled explicitly, stability ensures that, on average, passengers have the waiting time at an acceptable level. As mentioned above, vehicle routing problems are in general NP-hard. To avoid the computational inefficiency, Banerjee et al. (2016) studied shared vehicle systems from an approximation framework, which provided a relaxation approach for a range of objective functions.

Spieser et al. (2014) proposed a theoretical model to quantify the appropriate fleet size for AMoD systems by pointing out the importance of Earth mover's distance when constructing the relationship between minimum fleet size and average O-D distance. A numerical experiment using Singapore travel data found a replacement ratio of 3. Zhang et al. (2016b) extended the dispatch problem to congested road networks. They found that finding customers and rebalancing vehicles can be decoupled, but only under the assumption of specific cost functions and a symmetric road network. Also, they did not provide the optimal routing. Zhang et al. (2016a) used model predictive control to incorporate electric vehicle charging constraints to AMoD system. They proved their model converges to the optimal solution under a strong assumption that all passengers depart at the start of the study period. Kanoria and Qian (2019) proposed a so-called mirror backpressure control for a ridehailing platform. Their model uses no prior knowledge of the demand arrival rate and lacks a proof of stability, but their output is nearly optimal.

Concerns about the increased vehicle miles traveled (VMT) caused by rebalancing trips in AMoD systems and induced VMT due to the convenience of SAVs are also widely discussed. Simulations by Levin et al. (2017) and Maciejewski and Bischoff (2016) found that SAVs could greatly increase congestion due to increased VMT and un-optimized route choice. Levin (2017) proposed a linear program to minimize travel time for SAV service. Still, it requires future knowledge of demand. Zhang et al. (2016b) presented a network flow model for AMoD systems upon a capacity-symmetric network and found that appropriately arranging the rebalancing vehicles will not incur increased congestion. However, this analytical study was focused on the arrangement of idle trips only. Due to the complexity of analyzing the stability properties, we will exclude congestion from our model, like many previous studies. However, our model is sufficiently general to include congestion in future work.

Some researchers also tried to improve AMoD by extending the services that SAVs can provide. Autonomous vehicle sharing and reservation systems that ask passengers to request a ride ahead of time to arrange vehicle schedules in advance were studied by Ma et al. (2017). Ridesharing (serving multiple passengers simultaneously) has also been studied. Fagnant and Kockelman (2018) found that dynamic ridesharing plays a critical role to offset part of the VMT caused by relocation trips. Alonso-Mora et al. (2017) used a greedy algorithm and constrained optimization to solve the ridesharing problem extended to car-sharing and vans-sharing (i.e., extending each vehicle's occupant capacity). The results show that the current 13,000 taxis could be replaced by 3,000 taxis with a capacity of 4. Integrated SAVs with public transit systems are also expected to compensate for the first-/last-mile problem. Shen et al. (2018) built agent-based supply-side simulation with 52 scenarios considering various SAV fleet size and sharing preference. Moorthy et al. (2017) and Ohnemus and Perl (2016) discussed possible energy saving by shifting demand from other modes to automated last-mile transport (ALMT). Levin et al. (2019) explored the optimal integration by approximating passenger and vehicle movements through a linear program. Scheltes and de Almeida Correia (2017) explored the impact of pre-booking and higher speed limits for SAVs in ALMT systems. However, all of these studies used heuristic dispatch policies. Researchers also studied shared autonomous electric vehicle (SAEV) systems where electric AVs are implemented as a more energy-efficient automobile. Simulation work done by Chen et al. (2016) and Chen and Kockelman (2016) examined the charging infrastructure decision and pricing scheme problems, Iacobucci et al. (2018) and Zhang et al. (2016a) provided possible ways to incorporate charging constraints to current AMoD Models easily. Pricing policies for drivers and customers is another hot topic for shared vehicle systems (Ma et al., 2018; Kanoria and Qian, 2019; Banerjee et al., 2016), but the AMOD systems in our paper do not require drivers. Due to the analytical complexity, this paper will focus on the basic SAV problem without ridesharing, transit integration, or electric vehicles.

3. AMoD framework

In an AMoD system, passengers, a fleet of SAVs, and a central SAV dispatcher are the three main components activating on an AV-support network. Passengers send requests to the central SAV dispatcher via a mobile application to order a ride. Requests include basic travel information such as desired departure time, origin, and destination. A central SAV dispatcher is assumed to receive passengers' requests, know the status of all SAVs, and instruct SAVs to serve passengers according to the dispatch policy. Passengers are willing to be picked up instantaneously after sending out a request. We assume that each SAV serves one passenger request at a time, unlike ridesharing studies (Fagnant and Kockelman, 2018; Alonso-Mora et al., 2017; Levin et al., 2017). We make this assumption to simplify the model to admit analytical results.

Like most literature on this topic, parking space is assumed to be unlimited in this study. When a passenger requests pick-up, according to central SAV dispatcher's instruction, empty vehicles have three possible actions (or tasks) to perform at the current time step: pick up a passenger from the same zone immediately, relocate to another zone which has high demand and low supply, or stay parked in its current zone. Once a vehicle is assigned a task to pick up a passenger or relocate, it will be removed from the set of parked vehicles. Otherwise, it will stay and park at its current zone for the next time step. If a vehicle is removed from the parked fleet, it will not receive other assignments until arriving at the final destination of the current trip.

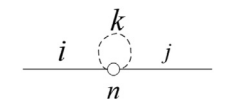


Fig. 1. Network definition.

Passengers are assumed to wait until picked up by an SAV. The average waiting time can be derived from the average behavior of the max-pressure dispatch policy (Corollary 1). As long as the demand is within the stable region, using the max-pressure dispatch policy prevents the queue from growing to infinity (Proposition 4) as the time goes to infinity. When an SAV finishes its current assignment, it will park at the terminal zone and await another trip assignment relocating or serving another passenger. Assume without loss of generality that each link has a constant travel time of one-time step (longer links can be separated into segments). In other words, the number of SAVs on the network will not affect traffic congestion. We retain the network structure so that future work can consider congestion effects from other vehicles or even from SAV interactions.

3.1. Network definition

Consider a traffic network $\mathscr{G} = (\mathscr{N}, \mathscr{A})$ with a set of nodes \mathscr{N} and set of links \mathscr{A} . SAVs travel through this network and interact with passengers as described above. Let $\mathscr{Z} \subset \mathscr{A}$ be the set of zones, which are a subset of the centroid links where SAVs park, enter, and exit to pick up/drop off passengers. Denote $\mathscr{A}_0 \subset \mathscr{A}$ as the set of non-zone links. Centroid links only represent the area where SAVs and passengers interact. In this study, pick-up and drop-off times are assumed to be zero. Thus, vehicles only have travel time on non-zone links. At each time step, SAVs can move forward through the non-zone links towards zones. Let Φ_i^s be the free flow shortest path travel time from i to s. In the example given in Fig. 1, link i and link j are non-zone links connected to node n, while link k is the centroid link.

link j are non-zone links connected to node n, while link k is the centroid link. Let Γ_i^+ and Γ_i^- be the sets of downstream and upstream links of link i, respectively. Let $x_j^{rs}(t)$ be the number of SAVs on link j traveling from $r \in \mathscr{Z}$ to $s \in \mathscr{Z}$ at time t. Let $y_{ij}^{rs}(t)$ be the number of SAVs going from r to s moving from link i to link j at time t. Then $x_i^{rs}(t)$ evolves via conservation:

$$x_j^{rs}(t+1) = x_j^{rs}(t) + \sum_{i \in \mathcal{A}} y_{ij}^{rs}(t) - \sum_{k \in \mathcal{A}} y_{jk}^{rs}(t)$$
 (1)

The variable $y_{ii}^{rs}(t)$ determine the route choice, and is constrained by SAVs on the link:

$$\sum_{k \in \Gamma^{+}} y_{jk}^{rs}(t) \le x_{j}^{rs}(t) \tag{2}$$

At zones, SAV interactions are slightly different. SAVs can change their origin and destination at zones. Let $p_r(t)$ be the number of SAVs parked at r at time t. Then

$$p_r(t+1) = p_r(t) + \sum_{i \in \mathcal{A}} \sum_{g \in \mathcal{Z}} y_{ir}^{qr}(t) - \sum_{i \in \mathcal{A}} \sum_{S \in \mathcal{Z}} y_{rj}^{rs}(t)$$
(3)

Exiting vehicles is constrained by the number of parked vehicles:

$$\sum_{j \in \mathscr{A}} \sum_{s \in \mathscr{Z}} y_{rj}^{rs}(t) \le p_r(t) \tag{4}$$

Notice that Eq. (4) includes an implicit constraint: SAV movements are limited by the fleet size $F \ge \sum_{r \in \mathscr{F}} p_r(0)$.

3.2. Passenger demand model

Let $d^{rs}(t)$ be the demand (number of new passengers) at time t wishing to travel from r to s. $d^{rs}(t)$ are random independent identically distributed variables with mean \bar{d}^{rs} . Let $w^{rs}(t)$ be the number of passengers waiting at r for travel to s. We use $\vec{d}(t)$ and $\vec{w}(t)$ to denote the vectors of demand and waiting passengers, respectively. Passengers will either be picked up or wait at r so $w^{rs}(t)$ evolves as follows:

$$w^{rs}(t+1) = w^{rs}(t) + d^{rs}(t) - \min\left\{ \sum_{j \in \mathcal{A}} y_{rj}^{rs}(t), w^{rs}(t) \right\}$$
 (5)

which also ensures that $w^{rs}(t) \ge 0$. Eq. (5) holds with probability 1. The minimum operation is because $\sum_{j \in \mathscr{A}} y^{rs}_{rj}(t)$ is the number of SAVs departing r to s at time t, and some of these SAVs may travel from r to s empty for rebalancing in response

to actual or predicted demand. The term $\min \left\{ \sum_{j \in \mathscr{A}} y_{rj}^{rs}(t), w^{rs}(t) \right\}$ represents the number of customer-carrying SAVs from r to s at time t.

Eq. (5) is based on the assumption that passengers will wait until they are picked up by a SAV. Our goal is to mathematically characterize the set of demand that can be served by a given fleet, and find an algorithm that can serve it (maximize throughput). If the fleet is permitted to ignore more costly origin-destination pairs (allowing the demand to leave due to a maximum waiting time) then the number of passengers served per hour per vehicle can be inflated by biasing the system against certain travelers. By forcing the fleet to serve all passengers, we believe we achieve a more accurate number for passengers served per vehicle, even if the traveler behavior is less accurate. Also, stability prevents queues from growing to infinity, which implicitly ensures the average waiting time will be bounded. This is proved in Section 4.5 Corollary 1. We leave for future work the notion of stability and the corresponding SAV dispatch behavior when passengers have a maximum waiting time.

3.3. Markov chain model

Given a dispatch policy, the constructed network model forms a Markov chain. The state is composed of the number of waiting passengers per origin-destination, $w^{rs}(t)$, the number of enroute vehicles at each node, $x_j^{rs}(t)$, and the number of parked vehicles at each node, $p_r(t)$. The transition functions are given by Eqs. (1), (3), and (5) where the stochasticity comes from the demand. The dispatch policy is represented by the variables $y_{ij}^{rs}(t)$. When the dispatch policy is a decision variable, the system becomes a Markov decision process. We will propose a specific dispatch policy and derive analytical results on the resulting Markov chain.

3.4. Max-pressure dispatch policy

We now define a max-pressure policy π^* , where the *pressure* is provided by the current numbers of waiting passengers. The max-pressure policy takes the form of a model predictive control algorithm. More specifically, at each time step t, the optimization program is solved and the optimal vehicle movement over the interval [t, t+T] is decided. Only the first control action (vehicle dispatch assignment at time t) will be actually executed. It will become clear from the proof of stability that this horizon is necessary for stability. Once a vehicle obtains an assignment, it will be removed from the parked fleet and no longer receive other assignments until it arrives its destination. Essentially, the central SAV dispatcher must plan ahead to rebalance vehicles as needed to satisfy current demand. This policy is established by solving the following linear program to allocate the fleet of SAVs to trips.

Let $f^{rs}(t)$ be the number of SAVs departing from r to s at time t. Let $v^{rs}(t)$ denote the number of customer-carrying vehicles from r to s at time t. $f^{rs}(t) \ge v^{rs}(t)$, but $f^{rs}(t)$ may be greater to accommodate empty SAV trips. The objective function consists of two parts. First, the main goal is to maximize the passenger throughput given a fixed fleet size. This is achieved by maximizing a pressure product $\sum_{(r,s)\in\mathscr{Z}^2} w^{rs}(t)v^{rs}(t+\tau)$ corresponding to the first term in Eq. (6). The reason for selecting this term will be explained in Section 4.5. We also wish to avoid unnecessary idle vehicles transversing through the network while ensure the number of customer-carrying vehicles are maximized. Thus, $-f^{rs}(t+\tau)$ is added to the objective function to reflect the aim to minimize vehicle movements, and the service trip $v^{rs}(t+\tau)$ is still maximized. Since we will only use the first control action at time t, and also we want to serve the passengers as soon as possible, we give a greater priority to service trips that move earlier via dividing $v^{rs}(t+\tau)$ by the time index τ . The later the time step, the smaller the value to the objective. On the other hand, lacking rebalancing trips also results in low throughput or unbounded waiting queue. Therefore, terms $-f^{rs}(t+\tau)$ and $\frac{v^{rs}(t+\tau)}{\tau}$ are multiplied by a small number λ to allow the queue lengths to dominate the objective once sufficiently large. These three terms are averaged by planning horizon T. Overall, the objective of the max-pressure dispatch policy is:

$$\max \frac{1}{T} \sum_{\tau=1}^{T} \sum_{(r,s) \in \mathscr{Z}^2} \left(w^{rs}(t) v^{rs}(t+\tau) - \lambda f^{rs}(t+\tau) + \lambda \frac{v^{rs}(t+\tau)}{\tau} \right)$$
 (6)

Note that at every time step t, $w^{rs}(t)$ is exogenous since t is fixed Section 4.5.

Vehicle locations and waiting passengers are constraints on this policy. The number of vehicles departing from r at time t should be upper bounded by the number of vehicles parked at r:

$$\sum_{s \in \mathscr{X}} f^{rs}(t+\tau) \le p_r(t+\tau) \qquad \forall r \in \mathscr{Z}, \forall \tau \in [0,T]$$
 (7)

By definition, the number of vehicles carrying passengers cannot exceed the number of vehicles traveling from that origin to that destination:

$$v^{rs}(t+\tau) \le f^{rs}(t+\tau)\forall (r,s) \in \mathcal{Z}^2, \forall \tau \in [0,T]$$
(8)

Notice that $p_r(t)$ is the number of SAVs parked at time step t, which is part of the state of the network. $p_r(t)$ will evolve deterministically over time depending on SAV trips and arriving vehicles, and the prediction is encoded as the constraint:

$$p_r(t+\tau+1) = p_r(t+\tau) + \sum_{q \in \mathcal{Z}} f^{qr}(t+\tau-\Phi^r_q) - \sum_{s \in \mathcal{Z}} f^{rs}(t+\tau) \qquad \forall r \in \mathcal{Z}, \forall \tau \in [0,T]$$
 (9)

The incoming flow, represented by the second term on the right-hand side of Eq. (9), is equivalent to trips that have remaining travel time equal to $t + \tau$, which is the number of vehicles that will arrive at r at time $t + \tau$. The third term in Eq. (9) is the outgoing flow from r at time $t + \tau$.

According to the model predictive control, given the parked fleet information at time t, we need to decide the optimal control sequence for time slots t to t+T, including when and where vehicles should travel/stay to serve the waiting queue at time t. Thus, passenger-carrying trips from t to t sum over planning horizon t should be less than the number of waiting passengers at time t:

$$\sum_{\tau=0}^{T} v^{rs}(t+\tau) \le w_{rs}(t) \forall (r,s) \in \mathcal{Z}^2$$

$$\tag{10}$$

Since $f^{rs}(t)$ is minimized in the objective function, we need to ensure flows are always non-negative, as shown in Eq. (11). $v^{rs}(t+\tau)$ should also be non-negative, as shown in Eq. (12).

$$f^{\mathsf{rs}}(t+\tau) \ge 0, \forall (r,s) \in \mathscr{Z}^2 \forall \tau \in [0,T] \tag{11}$$

$$v^{rs}(t+\tau) \ge 0, \forall (r,s) \in \mathcal{Z}^2 \forall \tau \in [0,T]$$
(12)

We now state the full linear program:

$$\max \frac{1}{T} \sum_{\tau=1}^{T} \sum_{(r,s) \in \mathscr{Z}^2} \left(w^{rs}(t) v^{rs}(t+\tau) - \lambda f^{rs}(t+\tau) + \lambda \frac{v^{rs}(t+\tau)}{\tau} \right)$$
s.t. constraints (7)–(12)

After solving linear program (13), assign $f^{rs}(t)$ vehicles to depart from r to s at time step t. The remainder of the solution is discarded. SAV assignments for time t+1 (and future times) will be re-optimized at the next time step using the updated realization of waiting passengers. Feasibility of future model outputs is guaranteed based on vehicle locations. Consistency of vehicle dispatch behaviors is also guaranteed because once dispatched, vehicles are not available for further control until they complete their trip. When the linear program considers a sufficiently long time horizon, relocation will be part of the optimal solution as it is necessary for serving passengers. A time horizon in excess of the maximum travel time between any two nodes should be sufficient for any relocation.

The second component of the policy is the route choice in the network. Recall that we assume that travel times are constant. Therefore, for every link i and every origin-destination pair (r,s), do the following: find a link j such that $\Phi_i^s > \Phi_j^s$ (which exists by definition of the shortest path). Set $y_{ij}^{rs}(t) = x_i^{rs}(t)$ to move all SAVs on i traveling from r to s to j. By always moving vehicles towards their destination, the travel time from r to s will always be equal to Φ_r^s . Notice that this includes the conversion of the $f^{rs}(t)$ variables to SAV departures in terms of $y_{ri}^{rs}(t)$ for some link $i \in \Gamma_r^+$. SAVs departing from r to s are routed onto a link i with $\Phi_s^s < \Phi_r^s$.

4. Proof of maximum stability

The main contribution of this paper is to prove the proposed max-pressure policy stabilizes the network whenever possible. We use Varaiya (2013)'s definition of stability, which is that the average expected number of waiting passengers remains bounded for every time T.

Definition 1. The stochastic queueing model is stable if there exists some $K < \infty$ such that

$$\mathbb{E}\left[\frac{1}{T}\sum_{t=1}^{T}\sum_{(r,s)\in\mathscr{Z}^2}w^{rs}(t)\right] \leq K \tag{14}$$

Theorem 2 of Leonardi et al. (2001) defines strong stability differently, which is actually equivalent to Definition 1:

Lemma 1. Suppose that there exists a value function $v(\vec{w}(t))$ satisfying $0 \le v(\vec{w}(t)) < \infty$ for all $\vec{w}(t)$ and

$$\mathbb{E}[\nu(\vec{w}(t+1)) - \nu(\vec{w}(t))|\vec{w}(t)] \le \kappa - \epsilon|\vec{w}(t)| \tag{15}$$

for all $\vec{w}(t)$ for some $\kappa < \infty$, $\epsilon > 0$. Then the queueing system satisfies the Definition 1 form of stability.

Proof. Uses part of the proof of Theorem 2 of Varaiya (2013). Taking the expectation on both sides of Eq. (15) and summing it over time T yields:

$$\sum_{t=1}^{T} \mathbb{E}[\nu(\vec{w}(t+1)) - \nu(\vec{w}(t))] \le \kappa T - \epsilon \sum_{t=1}^{T} |\mathbb{E}[\vec{w}(t)]|$$
(16)

Due to Eq. (5), the number of waiting passengers $\vec{w}(t)$ is non-negative. This enables the term on the right-hand side of Eq. (16) to change the order of expectation and absolute value function. Expand the summation on the left-hand side of equation (16) to obtain:

$$\mathbb{E}[\nu(\vec{w}(T+1))] - \mathbb{E}[\nu(\vec{w}(1))] \le \kappa T - \epsilon \sum_{t=1}^{T} \mathbb{E}[\vec{w}(t)]$$
(17)

Divide by T and rearrange terms to obtain:

$$\epsilon \frac{1}{T} \sum_{t=1}^{T} |\mathbb{E}[\vec{w}(t)]| \le \kappa + \frac{1}{T} \mathbb{E}[\nu(\vec{w}(1))] - \frac{1}{T} \mathbb{E}[\nu(\vec{w}(T+1))]$$

$$\tag{18}$$

$$\leq \kappa + \frac{1}{T} \mathbb{E}[\nu(\vec{w}(1))] \tag{19}$$

which implies stability condition (14). \Box

4.1. Stable region

For any given fleet size, it is easily possible to find an average demand rate that cannot be stabilized. If the demand is sufficiently high, no SAV dispatch policy will be able to serve all passengers. Therefore it is necessary to characterize the *stable region* of demand given a fleet size. Stable region is the set of demand that could be served by a given fleet size under *any* dispatch policy. We then show that the max-pressure policy will stabilize any demand within the stable region.

Let \bar{y}_{ij}^{rs} be an average rate of SAV flow from link i to link j from origin r to destination s, and let \overrightarrow{y} be the average flow vector. The system is stable if there exists \bar{y}_{ij}^{rs} satisfying the following constraints. First, the sum of the average flows cannot exceed the fleet size, which is denoted as F.

$$\sum_{(\mathbf{r},\mathbf{s})\in\mathscr{Z}^2} \sum_{(i,j)\in\mathscr{A}^2} \vec{y}_{ij}^{rs} \le F \tag{20}$$

Flow must be conserved on non-zone links, i.e. the number of SAVs entering a non-zone link is equal to the number of SAVs exiting.

$$\sum_{i \in \Gamma_{i}^{-}} \bar{y}_{ij}^{rs} = \sum_{k \in \Gamma_{i}^{+}} \bar{y}_{jk}^{rs} \qquad \qquad \forall (r, s) \in \mathcal{Z}^{2}, \forall j \in \mathcal{A}_{0}$$
 (21)

Conservation of flow on centroid links is different from the conservation of flow on non-zone links because SAV destinations can change:

$$\sum_{q \in \mathcal{Z}} \sum_{i \in \Gamma_r^-} \bar{y}_{ir}^{qr} = \sum_{s \in \mathcal{Z}} \sum_{j \in \Gamma_r^+} \bar{y}_{rj}^{rs} \qquad \forall r \in \mathcal{Z}$$
(22)

Let $\bar{\mathscr{Y}}$ be the set of average SAV assignments that \vec{y} satisfying constraints (20)–(22). $\bar{\mathscr{Y}}$ is the feasible set of stationary SAV dispatch assignments. The last constraint defining the stable region is to satisfy all demand:

$$\sum_{i \in \Gamma^{\pm}} \bar{y}_{ri}^{rs} \ge d^{rs} \qquad \qquad \forall (r, s) \in \mathscr{Z}^2$$
 (23)

Let $\mathscr{D} = \{\vec{d} : \exists \vec{y} \in \mathscr{Y} \text{ satisfying constraint (23)} \}$, and let \mathscr{D}^0 be the interior of \mathscr{D} . The difference between \mathscr{D} and \mathscr{D}^0 is that constraints (20) and (23) can hold with equality in \mathscr{D} , but must be strictly inequalities in \mathscr{D}^0 . If some average demand is on the boundary of \mathscr{D} , any dispatch policy will result in a null recurrent Markov chain. In other words, an arbitrarily large queue length will eventually be reduced, but the expected time required is infinite.

Using the stable region, we can prove analytically that a replacement ratio exists and is independent of the fleet size. Equivalently, increasing the fleet size will proportionally increase the number of passengers that can be served.

Proposition 1. The maximum demand $\sum_{(r,s)\in\mathscr{Z}^2} \bar{d}^{rs}$ that a fleet with size F can serve will increase proportionally with respect to the increase of F.

Proof. Consider a fleet of SAVs with size F. Combining constraints (20)–(23):

$$\beta \sum_{r \in \mathscr{Z}} \sum_{s \in \mathscr{Z}} d^{rs} \le \beta \sum_{r \in \mathscr{Z}} \sum_{s \in \mathscr{Z}} \sum_{i \in \Gamma_r^+} \bar{y}_{ri}^{rs} = \beta \sum_{r \in \mathscr{Z}} \sum_{q \in \mathscr{Z}} \sum_{i \in \Gamma_r^-} \bar{y}_{ir}^{qr} \le \beta F$$

$$(24)$$

Multiplying F by a factor of β admits a β change in $\sum_{(r,s)\in \mathscr{Z}'^2} \bar{d}^{rs}$ also. \square

Proposition 2. If $\vec{d} \notin \mathcal{D}$, then the system cannot be stabilized by any $\overrightarrow{y} \in \mathcal{Y}$.

Proof. For every $\overrightarrow{y} \in \overline{\mathscr{Y}}$ there exists some $(r,s) \in \mathscr{Z}^2$ such that $\sum_{i \in \Gamma_r^+} \vec{y}_{ri}^{rs} - \bar{d}^{rs} \ge \eta$ for some $\eta > 0$. Then on average, $w^{rs}(t)$

will increase by η per time step, for a total of ηT over a time horizon of T. As $T \to \infty$, the number of waiting passengers will also increase to ∞ which violates Definition 1 for stability. \square

Proposition 2 shows that if $\vec{d} \notin \mathcal{D}$, then a larger fleet size is needed to serve all demand. Equivalently, if the max-pressure policy is stable for all demand in \mathcal{D} , then it will have *maximum stability*. Notice that the minimum fleet size to satisfy (20)–(23) can be determined using a linear program:

$$\min \qquad F = \epsilon + \sum_{(r,s) \in \mathscr{Z}^2} \sum_{(i,j) \in \mathscr{Z}^2} \bar{y}_{ij}^{rs} \tag{25a}$$

s.t.
$$\sum_{q \in \mathcal{Z}} \sum_{i \in \Gamma_r^-} \bar{y}_{ir}^{qr} = \sum_{s \in \mathcal{Z}} \sum_{j \in \Gamma_r^+} \bar{y}_{jr}^{rs} \qquad \forall r \in \mathcal{Z}$$
 (25b)

$$\sum_{i \in \Gamma_i^-} \bar{y}_{ij}^{rs} = \sum_{j \in \Gamma_i^+} \bar{y}_{jk}^{rs} \qquad \forall (r, s) \in \mathcal{Z}^2, \forall j \in \mathcal{A}_0$$
 (25c)

$$\sum_{i \in \Gamma^+} \bar{y}_{ri}^{rs} \ge \bar{d}^{rs} + \epsilon \qquad \qquad \forall (r, s) \in \mathcal{Z}^2$$
 (25d)

$$\bar{y}_{ii}^{rs} \ge 0$$
 $\forall (r,s) \in \mathcal{Z}^2, \forall (i,j) \in \mathcal{A}^2$ (25e)

where $\epsilon > 0$ is the buffer to ensure that constraints (20) and (23) are strict inequalities. The size of the buffer desired is exogenous, but it will become apparent in the proof of stability that a smaller buffer requires a larger planning horizon. Linear program (25) admits stochastic demand with any distribution, as long as the mean demands per origin-destination \bar{d}^{rs} are known.

4.2. Minimum length of the planning horizon T in π^*

To connect \bar{y} with actual SAV movements, it is necessary to show that there exists a sequence of SAV dispatch assignments that will result in stationary average flows of \bar{y} . This sequence will also become useful in the proof of stability. The minimum length of the planning horizon T in π^* is based on how close the sequence needs to approximate \bar{y} , which will be seen in Section 4.5.

Proposition 3. There exists a sequence $\vec{y}(t)$ such that

$$\lim_{T \to \infty} \frac{1}{T} \sum_{t=0}^{T} \overrightarrow{y}(t) = \overline{\overrightarrow{y}}$$
 (26)

for any $\vec{p}(0)$, $\vec{x}(0)$ satisfying

$$\sum_{r \in \mathscr{Z}} p_r(0) + \sum_{(r,s) \in \mathscr{Z}^2} \sum_{i \in \mathscr{A}} x_i^{rs}(0) = F$$

$$\tag{27}$$

Proof. For any $\epsilon > 0$ and for all $(i, j) \in \mathscr{A}^2$, $(r, s) \in \mathscr{Z}^2$, there exists rational numbers $\gamma_{ij}^{rs} \in \mathbb{Q}$ such that $|\vec{y}_{ij}^{rs} - \gamma_{ij}^{rs}| < \epsilon$ with \vec{y} satisfying constraints (21) and (22) because there is a rational number between any two different real numbers. Let K_1 be the least common multiple of the denominators of all γ_{ij}^{rs} , then assuming the correct starting positions of vehicles, there exists a $\vec{y}(t)$ such that

$$\sum_{t=0}^{K_1} \vec{y}(t) = \vec{\gamma} K_1, \tag{28}$$

since $\vec{\gamma}K_1$ is integer and satisfies the conservation of flow at centroid links and other nodes from constraints (21) and (22). For $T > K_1$, repeating the $\vec{y}(t)$ assignment will also yield $\vec{\gamma}K_1$. Moving the vehicles to their starting locations requires at most $K_2 = \max_{(r,s) \in \mathbb{Z}^2} \{\Phi_r^s\}$ time (to satisfy the assumption about the correct starting positions), so there exists a $\vec{y}(t)$ that is at

most ϵ away from \overrightarrow{y} after $K_1 + K_2$ time. \square

Given a fixed (lookahead) time horizon $T \in \mathbb{N}$, the $\vec{y}(t)$ that has the minimum difference between a \vec{y} that is sufficient for demand $\vec{d} \in \mathcal{D}^0$ can be found by solving the following quadratic program:

$$\min \sum_{(i,j)\in\mathscr{A}^2} \sum_{(r,s)\in\mathscr{Z}^2} \left(\bar{y}_{ij}^{rs} - \frac{1}{T} \sum_{t=0}^T y_{ij}^{rs}(t) \right)^2 \tag{29a}$$

s.t.
$$\sum_{i \in \mathscr{A}} y_{ij}^{rs}(t) \le x_i^{rs}(t)$$

$$\forall (r,s) \in \mathscr{Z}^2, \forall i \in \mathscr{A}_0, \forall t \in [0,T]$$
 (29b)

$$x_j^{rs}(t+1) = x_j^{rs}(t) + \sum_{i \in \mathcal{A}} y_{ij}^{rs}(t) - \sum_{k \in \mathcal{A}} y_{jk}^{rs}(t) \qquad \qquad \forall (r,s) \in \mathcal{Z}^2, \forall j \in \mathcal{A}_0, \forall t \in [0,T]$$

$$(29c)$$

$$p_r(t+1) = p_r(t) + \sum_{q \in \mathcal{Z}} \sum_{i \in \mathcal{A}} y_{ir}^{qr}(t) - \sum_{s \in \mathcal{Z}} \sum_{j \in \mathcal{A}} y_{rj}^{rs}(t) \qquad \forall r \in \mathcal{Z}, \forall t \in [0, T]$$
 (29d)

$$y_{ij}^{rs}(t) \ge 0$$
 $\forall (r,s) \in \mathscr{Z}^2, \forall (i,j) \in \mathscr{A}^2, \forall t \in [0,T]$ (29e) constraints (20)–(23)

with $\vec{p}(0)$ given. Notice that \overrightarrow{y} is also a decision variable in program (29) because there may be multiple $\overrightarrow{y} \in \overline{\mathscr{Y}}$ that are sufficient for the demand \overrightarrow{d} . Unfortunately, if T is a decision variable, the optimization problem is no longer quadratic. Still, since T has a single dimension, the minimum value needed to obtain an ϵ level of precision can be found through a binary search.

4.3. Analytical method for finding the replacement ratio

The definition of replacement ratio is: the number of passengers served by one SAV per unit time. Mathematically, the replacement ratio is defined as $\frac{\sum\limits_{(f,s)\in \mathscr{Z}^2}\tilde{d}^{fs}}{F}$. Therefore, the maximum replacement ratio could be found by solving the following linear program:

$$\max \frac{\sum\limits_{(r,s)\in\mathscr{Z}^2} \bar{d}^{rs}}{F}$$
s.t. constraints (20) – (23)

Notice this ratio ignores the origin-destination demand proportions. The highest replacement ratios will be achieved for symmetric demand, which does not require empty rebalancing. The origin-destination demand proportions can be included in problem (30) by adding the following constraint:

$$\bar{d}^{rs} = \alpha^{rs} \sum_{(r,s) \in \mathscr{Z}^2} \bar{d}^{rs} \qquad \qquad \forall (r,s) \in \mathscr{Z}^2$$
 (31)

where α^{rs} is the proportion of total demand that travels from r to s. Thus, the replacement ratio should be solved with the knowledge of demand pattern by adding Eq. (31) to linear program (30).

4.4. Preliminary stability results

To assist with the proof of stability for the max-pressure policy, we first state and prove two lemmas related to the dispatching policy using the average flow \bar{y} . Then, we prove that the max-pressure dispatch policy performs better than \bar{y} . Because SAV rebalancing requires time to take effect, large realizations of stochastic demand will result in a correspondingly large number of waiting passengers that may not be reduced for some time.

Lemma 2. Consider the Lyapunov function $v(\vec{w}(t)) = |\vec{w}(t)|^2 = \sum_{(r,s)\in\mathscr{Z}^2} (w^{rs}(t))^2$. If $\vec{d} \in \mathscr{D}^0$ and the dispatch policy uses average

flow $\overline{\vec{y}}$, there exists an $\epsilon > 0$ and a $\kappa < \infty$ such that

$$\mathbb{E}[\nu(\vec{w}(t+1)) - \nu(\vec{w}(t))|\vec{w}(t)] \le \kappa - \epsilon|\vec{w}(t)| \tag{32}$$

Proof. The Lyapunov function is $\nu(\vec{w}(t)) = \sum_{(r,s) \in \mathscr{X}^2} (w^{rs}(t))^2$. Equivalently, we need to show that

$$\mathbb{E}\left[\sum_{(r,s)\in\mathscr{Z}^2} \left(\left(w^{rs}(t+1) \right)^2 - \left(w^{rs}(t) \right)^2 \right) |\vec{w}(t)| \right] \le \kappa - \epsilon |\vec{w}(t)| \tag{33}$$

for some $\kappa < \infty$ and some $\epsilon > 0$. Let $\delta^{rs}(t) = w^{rs}(t+1) - w^{rs}(t)$. According to Eq. (5), $\delta^{rs}(t)$ can also be written as:

$$\delta^{rs}(t) = w^{rs}(t+1) - w^{rs}(t) = d^{rs}(t) - \min\left\{w^{rs}(t), \sum_{i \in \mathcal{A}} \bar{y}_{ri}^{rs}(t)\right\}$$
(34)

Making the substitution $w^{rs}(t+1) = \delta^{rs}(t) + w^{rs}(t)$,

$$\mathbb{E}\left[\sum_{(r,s)\in\mathscr{Z}^2} \left(w^{rs}(t+1)\right)^2 - \left(w^{rs}(t)\right)^2 |\vec{w}(t)\right] = \mathbb{E}\left[\sum_{(r,s)\in\mathscr{Z}^2} \left(\delta^{rs}(t)\right)^2 + 2w^{rs}(t)\delta^{rs}(t)|\vec{w}(t)\right]$$
(35)

Let \widetilde{w}^{rs} be the maximum possible service rate from origin r to destination s, and \widetilde{d}^{rs} be the maximum value of random demand from origin r to destination s. From Eq. (34), we have the following bounds on $\delta^{rs}(t)$:

$$\delta^{rs}(t) \le \max\left\{\widetilde{w}^{rs}, \widetilde{d}^{rs}\right\} \qquad \qquad \forall (r, s) \in \mathscr{Z}^2 \tag{36}$$

Let K be the maximum value of all bounds considering all $(r, s) \in \mathcal{Z}^2$,

$$K = \max_{(r,s) \in \mathcal{Z}^2} \left\{ \max \left\{ \widetilde{w}^{rs}, \widetilde{d}^{rs} \right\} \right\}. \tag{37}$$

Then $(\delta^{rs}(t))^2 \le K^2$ for all $(r,s) \in \mathcal{Z}^2$ which achieves

$$\sum_{(r,s)\in\mathscr{Z}^2} (\delta^{rs}(t))^2 \le mK^2 \tag{38}$$

where m is the total number of pairs of origin and destination. Taking the expectation on both sides, we have

$$\mathbb{E}\left[\sum_{(r,s)\in\mathscr{Z}^2} \left(\delta^{rs}(t)\right)^2\right] \le mK^2 \tag{39}$$

 mK^2 can be represented by κ in Eq. (32), which leaves $\mathbb{E}\left[\sum_{(r,s)\in\mathscr{Z}^2} 2w^{rs}(t)\delta^{rs}(t)|\vec{w}(t)\right]$ from Eq. (35). Plug Eq. (34) into this remaining term to obtain,

$$\mathbb{E}\left[\sum_{(r,s)\in\mathscr{Z}^2} 2w^{rs}(t)\delta^{rs}(t)|\vec{w}(t)\right]$$

$$= \mathbb{E}\left[\sum_{(r,s)\in\mathscr{Z}^2} 2w^{rs}(t)\left(\bar{d}^{rs} - \min\left\{w^{rs}(t), \sum_{i\in\mathscr{A}} \bar{y}^{rs}_{ri}(t)\right\}\right)|\vec{w}(t)\right]$$

$$= \sum_{(r,s)\in\mathscr{Z}^2} 2w^{rs}(t)\left(\bar{d}^{rs} - \min\left\{w^{rs}(t), \sum_{i\in\mathscr{A}} \bar{y}^{rs}_{ri}(t)\right\}\right)$$

If $w^{rs}(t) \leq \sum_{i \in \mathscr{A}} \bar{y}^{rs}_{ri}(t)$, the waiting passengers will be served by the flow out. Otherwise, if $w^{rs}(t) \geq \sum_{i \in \mathscr{A}} \bar{y}^{rs}_{ri}(t)$,

$$\min \left\{ w^{rs}(t), \sum_{i \in \mathcal{A}} \bar{y}_{ri}^{rs}(t) \right\} = \sum_{i \in \mathcal{A}} \bar{y}_{ri}^{rs}(t):$$

$$\sum_{(r,s)\in\mathscr{Z}^2} 2w^{rs}(t) \left(\bar{d}^{rs} - \min\left\{ w^{rs}(t), \sum_{i\in\mathscr{A}} \bar{y}^{rs}_{ri}(t) \right\} \right) = \sum_{(r,s)\in\mathscr{Z}^2} 2w^{rs}(t) \left(\bar{d}^{rs} - \sum_{i\in\mathscr{A}} \bar{y}^{rs}_{ri}(t) \right)$$

$$\tag{40}$$

Because $\bar{d} \in \mathcal{D}^0$, there exists an $\epsilon > 0$ such that $\bar{d}^{rs} - \sum_{i \in \mathcal{A}} \bar{y}_{ri}^{rs} \leq -\epsilon$. Then

$$\sum_{(r,s)\in\mathscr{Z}^2} 2w^{rs}(t) \left(\bar{d}^{rs} - \sum_{i\in\mathscr{A}} \bar{y}^{rs}_{ri} \right) \le -\epsilon \sum_{(r,s)\in\mathscr{Z}^2} w^{rs}(t) \le -\epsilon |\vec{w}(t)| \tag{41}$$

П

which results in

$$\mathbb{E}[\nu(\vec{w}(t+1)) - \nu(\vec{w}(t))] \le \kappa - \epsilon |\vec{w}(t)| \tag{42}$$

Lemma 3. For any control $\vec{y}(t)$ and any $T \in \mathbb{N}$, if there exists $\kappa_1 < \infty$ and $\epsilon > 0$ such that

$$\mathbb{E}\left[\sum_{(r,s)\in\mathscr{Z}^2} (w^{rs}(t+1))^2 - (w^{rs}(t))^2 \middle| \vec{w}(t) \right] \le \kappa_1 - \epsilon |\vec{w}(t)| \tag{43}$$

then there exists $\kappa_2 < \infty$ such that

$$\frac{1}{T} \sum_{\tau=1}^{T} \mathbb{E} \left[\sum_{(r,s) \in \mathscr{Z}^2} (w^{rs}(t+\tau+1))^2 - (w^{rs}(t+\tau))^2 \middle| \vec{w}(t+\tau) \right] \le \kappa_2 - \epsilon |\vec{w}(t)|$$
(44)

Proof. By Eq. (43),

$$\frac{1}{T} \sum_{\tau=1}^{T} \mathbb{E} \left[\sum_{(r,s) \in \mathcal{Z}^2} (w^{rs}(t+\tau+1))^2 - (w^{rs}(t+\tau))^2 \middle| \vec{w}(t+\tau) \right] \le \frac{1}{T} \sum_{\tau=1}^{T} \kappa_1 - \epsilon \middle| \vec{w}(t+\tau) \middle|$$
(45)

$$\leq \frac{1}{T} \sum_{\tau=1}^{T} \left(\kappa_1 - \epsilon \sum_{(r,s) \in \mathcal{Z}^2} (w^{rs}(t) - \tau F) \right) \tag{46}$$

$$\leq \kappa_2 - \epsilon \sum_{(r,s)\in\mathscr{Z}^2} (w^{rs}(t)) \tag{47}$$

$$= \kappa_2 - \epsilon |\vec{w}(t)| \tag{48}$$

 $w^{rs}(t+\tau) - w^{rs}(t) \ge -\tau F$ since at most F passengers can depart r per time step. \Box

4.5. Maximum stability of the max-pressure dispatch policy

We are now ready to prove the maximum stability property of the proposed max-pressure dispatch policy. The main results are included in Lemma 4:

Lemma 4. When the max-pressure policy is used with $\bar{d}' \in \mathcal{D}^0$, there exists a M such that for all (lookahead) time horizons T > M,

$$\mathbb{E}\left[\frac{1}{T}\sum_{\tau=1}^{T}\sum_{(r,s)\in\mathscr{Z}^{2}}(w_{rs}(t+\tau+1))^{2}-(w_{rs}(t+\tau))^{2}\middle|\vec{w}(t)\right] \leq \kappa-\epsilon|\vec{w}(t)|\tag{49}$$

Proof. Choose the value function $\nu(\vec{w}(t)) = \sum_{(r,s) \in \mathscr{Z}^2} (w^{rs}(t))^2$. We will show that the π^* policy performs better than any

feasible control \hat{y} . In Proposition 3, we already proved that as long as the time horizon T is greater than certain threshold, the sequence of dispatch assignments using the average flow \bar{y} can be estimated by a sequence of feasible control \hat{y} . Next, if we can prove the max-pressure control policy π^* outperforms all other feasible controls, in which \hat{y} is one of the feasible controls, then, it is obvious that π^* outperforms \hat{y} (which converges to \bar{y}). According to Lemma 2, we have proved that the dispatch policy using average flow \bar{y} leads to Eq. (32). Further, by Lemma 1, the dispatching policy using \bar{y} satisfies the Definition 1 form of stability. If the max-pressure dispatch policy π^* outperforms the one using \bar{y} , then the max-pressure dispatch policy is also stable. Now we are going to show that π^* outperforms \hat{y} :

$$\mathbb{E}\left[\frac{1}{T}\sum_{\tau=1}^{T}\sum_{(r,s)\in\mathscr{Z}^{2}}(w^{rs}(t+\tau+1))^{2}-(w^{rs}(t+\tau))^{2}|\vec{w}(t)\right] \leq \kappa-\epsilon|\vec{w}(t)|$$
(50)

for some $T < \infty$ and some $\epsilon > 0$. Let

$$\delta^{rs}(t) = w^{rs}(t+1) - w^{rs}(t) = d^{rs}(t) - \min\left\{w^{rs}(t), \sum_{i \in \mathcal{A}} y_{ri}^{rs}(t)\right\}$$
 (51)

Making the substitution $w^{rs}(t+1) = \delta^{rs}(t) + w^{rs}(t)$,

$$\mathbb{E}\left[\frac{1}{T}\sum_{\tau=1}^{T}\sum_{(r,s)\in\mathscr{Z}^{2}}(w^{rs}(t+\tau+1))^{2}-(w^{rs}(t+\tau))^{2}|\vec{w}(t)\right]$$

$$=\mathbb{E}\left[\frac{1}{T}\sum_{\tau=1}^{T}\sum_{(r,s)\in\mathscr{Z}^{2}}(\delta^{rs}(t+\tau))^{2}+2w^{rs}(t+\tau)\delta^{rs}(t+\tau)|\vec{w}(t)\right]$$
(52)

As shown in the proof of Lemma 2.

$$\mathbb{E}\left[\frac{1}{T}\sum_{\tau=1}^{T}\sum_{(r,s)\in\mathscr{Z}^2}\left(\delta^{rs}(t+\tau)\right)^2\right] \leq mK^2\tag{53}$$

which leaves $\mathbb{E}\left[\frac{1}{T}\sum_{\tau=1}^{T}\sum_{(r,s)\in\mathscr{Z}^2}2w^{rs}(t+\tau)\delta^{rs}(t+\tau)|\vec{w}(t)\right]$ from Eq. (52). Plug Eq. (51) into this remaining term to obtain

$$\mathbb{E}\left[\frac{1}{T}\sum_{\tau=1}^{T}\sum_{(r,s)\in\mathscr{Z}^{2}}2w^{rs}(t+\tau)\delta^{rs}(t+\tau)|\vec{w}(t)\right]$$

$$=\mathbb{E}\left[\frac{1}{T}\sum_{\tau=1}^{T}\sum_{(r,s)\in\mathscr{Z}^{2}}2w^{rs}(t+\tau)\left(\bar{d}^{rs}-\min\left\{w^{rs}(t+\tau),\sum_{i\in\mathscr{A}}y_{ri}^{rs}(t+\tau)\right\}\right)|\vec{w}(t)\right]$$
(54)

We can rewrite $w^{rs}(t+\tau)$ with respect to $w^{rs}(t)$ as:

$$w^{rs}(t+\tau) = \tau d^{rs} - \sum_{\tau'=1}^{T} \min \left\{ w^{rs}(t+\tau'), \sum_{i \in \mathscr{A}} y_{ri}^{rs}(t+\tau') \right\}$$
 (55)

Eq. (54) can be further expanded as:

$$\mathbb{E}\left[\frac{1}{T}\sum_{\tau=1}^{T}\sum_{(r,s)\in\mathscr{Z}^{2}}2w^{rs}(t+\tau)\delta^{rs}(t+\tau)|\vec{w}(t)\right]$$

$$=\mathbb{E}\left[\frac{1}{T}\sum_{\tau=1}^{T}\sum_{(r,s)\in\mathscr{Z}^{2}}2w^{rs}(t+\tau)\left(\bar{d}^{rs}-\min\left\{w^{rs}(t+\tau),\sum_{i\in\mathscr{A}}y_{ri}^{rs}(t+\tau)\right\}\right)|\vec{w}(t)\right]$$

$$=\frac{1}{T}\sum_{\tau=1}^{T}\sum_{(r,s)\in\mathscr{Z}^{2}}2\left(w^{rs}(t)+\tau\bar{d}^{rs}\right)\left(\bar{d}^{rs}-\min\left\{w^{rs}(t+\tau),\sum_{i\in\mathscr{A}}y_{ri}^{rs}(t+\tau)\right\}\right)$$

$$-\frac{1}{T}\sum_{\tau=1}^{T}\sum_{(r,s)\in\mathscr{Z}^{2}}\left(\sum_{\tau'=1}^{T}\min\left\{w^{rs}(t+\tau'),\sum_{i\in\mathscr{A}}y_{ri}^{rs}(t+\tau')\right\}\right)\left(\bar{d}^{rs}-\min\left\{w^{rs}(t+\tau),\sum_{i\in\mathscr{A}}y_{ri}^{rs}(t+\tau)\right\}\right)$$
(56)

Here, $\min \left\{ w^{rs}(t+\tau), \sum_{i \in \mathscr{A}} y^{rs}_{ri}(t+\tau) \right\}$ is the number of customer-carrying trips at time $t+\tau$, corresponding to the control variable $v^{rs}(t+\tau)$ in problem (13). $\bar{d}^{rs} - \min \left\{ w^{rs}(t+\tau), \sum_{i \in \mathscr{A}} y^{rs}_{ri}(t+\tau) \right\}$ is upper bounded by \bar{d}^{rs} , while the number of

trol variable $v^{rs}(t+\tau)$ in problem (13). $\bar{d}^{rs} - \min \left\{ w^{rs}(t+\tau), \sum_{i \in \mathscr{A}} y_{ri}^{rs}(t+\tau) \right\}$ is upper bounded by \bar{d}^{rs} , while the number of customer-carrying trips over time horizon [t, t+T] is bounded by the fleet size F. Thus, the second term on the right-hand side of Eq. (56) can be upper bounded as:

$$\frac{1}{T} \sum_{\tau=1}^{T} \sum_{(r,s) \in \mathcal{Z}^2} \sum_{\tau'=1}^{T} \min \left\{ w^{rs}(t+\tau'), \sum_{i \in \mathcal{A}} y_{ri}^{rs}(t+\tau') \right\} \left(\bar{d}^{rs} - \min \left\{ w^{rs}(t+\tau), \sum_{i \in \mathcal{A}} y_{ri}^{rs}(t+\tau) \right\} \right)$$

$$\leq F \sum_{(r,s) \in \mathcal{Z}^2} \bar{d}^{rs} \tag{57}$$

 $F \sum_{(r,s) \in \mathscr{Z}^2} \bar{d}^{rs}$ is again a constant value, which can be represented by κ in Eq. (50). The first term of Eq. (56) can be written in two parts:

$$\frac{1}{T} \sum_{\tau=1}^{T} \sum_{(r,s) \in \mathscr{Z}^2} 2 \left(w^{rs}(t) + \tau \bar{d}^{rs} \right) \left(\bar{d}^{rs} - \min \left\{ w^{rs}(t+\tau), \sum_{i \in \mathscr{A}} y^{rs}_{ri}(t+\tau) \right\} \right)$$

$$= \frac{1}{T} \sum_{\tau=1}^{T} \sum_{(r,s) \in \mathcal{Z}^2} 2w^{rs}(t) \left(\bar{d}^{rs} - \min \left\{ w^{rs}(t+\tau), \sum_{i \in \mathcal{A}} y^{rs}_{ri}(t+\tau) \right\} \right)$$

$$+ \frac{1}{T} \sum_{\tau=1}^{T} \sum_{(r,s) \in \mathcal{Z}^2} 2\tau \bar{d}^{rs} \left(\bar{d}^{rs} - \min \left\{ w^{rs}(t+\tau), \sum_{i \in \mathcal{A}} y^{rs}_{ri}(t+\tau) \right\} \right)$$
(58)

where the second term on the right-hand side of Eq. (58) is bounded by:

$$\frac{1}{T} \sum_{\tau=1}^{T} \sum_{(r,s) \in \mathcal{Z}^2} 2\tau \bar{d}^{rs} \left(\bar{d}^{rs} - \min \left\{ w^{rs}(t+\tau), \sum_{i \in \mathcal{A}} y^{rs}_{ri}(t+\tau) \right\} \right) \le 2T \sum_{(r,s) \in \mathcal{Z}^2} \left(\bar{d}^{rs} \right)^2$$

$$(59)$$

This is because τ can be upper bounded by T and $\bar{d}^{rs} - \min\left\{w^{rs}(t+\tau), \sum\limits_{i\in\mathscr{A}}y^{rs}_{ri}(t+\tau)\right\}$ can be upper bounded by \bar{d}^{rs} . This leaves the first term $\frac{1}{T}\sum_{\tau=1}^{T}\sum\limits_{(r,s)\in\mathscr{Z}^2}2w^{rs}(t)\left(\bar{d}^{rs} - \min\left\{w^{rs}(t+\tau), \sum\limits_{i\in\mathscr{A}}y^{rs}_{ri}(t+\tau)\right\}\right)$ on the right-hand side of Eq. (58). Note that $\min\left\{w^{rs}(t+\tau), \sum\limits_{i\in\mathscr{A}}y^{rs}_{ri}(t+\tau)\right\}$ is denoted as $v^{rs}(t+\tau)$ and $v^{rs}(t+\tau)$ is denoted as $v^{rs}(t+\tau)$ in problem (13). $v^{rs}(t+\tau)$ is the first term of the objective function in problem (13). To adjust

our proof to the objective function in problem (13), we add terms $-\lambda \sum_{i \in \mathscr{A}} y_{ri}^{rs\star}(t+\tau) + \lambda \frac{\min\left\{w^{rs}(t+\tau), \sum_{i \in \mathscr{A}} y_{ri}^{rs\star}(t+\tau)\right\}}{\tau}$ to term $w^{rs}(t) \min\left\{w^{rs}(t+\tau), \sum_{i \in \mathscr{A}} y_{ri}^{rs\star}(t+\tau)\right\}$. By solving problem (13), we have

$$\frac{1}{T} \sum_{\tau=1}^{T} \sum_{(r,s) \in \mathcal{Z}^{2}} \left(w^{rs}(t) \min \left\{ w^{rs}(t+\tau), \sum_{i \in \mathcal{A}} y^{rs\star}_{ri}(t+\tau) \right\} - \lambda \sum_{i \in \mathcal{A}} y^{rs\star}_{ri}(t+\tau) + \lambda \frac{\min \left\{ w^{rs}(t+\tau), \sum_{i \in \mathcal{A}} y^{rs\star}_{ri}(t+\tau) \right\}}{\tau} \right) \\
\geq \frac{1}{T} \sum_{\tau=1}^{T} \sum_{(r,s) \in \mathcal{Z}^{2}} \left(w^{rs}(t) \min \left\{ w^{rs}(t+\tau), \sum_{i \in \mathcal{A}} \hat{y}^{rs}_{ri}(t+\tau) \right\} - \lambda \sum_{i \in \mathcal{A}} \hat{y}^{rs}_{ri}(t+\tau) + \lambda \frac{\min \left\{ w^{rs}(t+\tau), \sum_{i \in \mathcal{A}} \hat{y}^{rs}_{ri}(t+\tau) \right\}}{\tau} \right) \right) \tag{60}$$

Also, terms $\frac{1}{T}\sum_{\tau=1}^{T}\sum_{(r,s)\in\mathscr{X}^2} -\lambda\sum_{i\in\mathscr{A}}y_{ri}^{rs}(t+\tau) + \lambda\frac{\min\left\{w^{rs}(t+\tau),\sum\limits_{i\in\mathscr{A}}y_{ri}^{rs}(t+\tau)\right\}}{\tau}$ in Eq. (60) are bounded as follows:

$$\frac{1}{T} \sum_{\tau=1}^{T} \sum_{(r,s) \in \mathscr{Z}^2} \lambda \frac{\min\left\{ w^{rs}(t+\tau), \sum_{i \in \mathscr{A}} y_{ri}^{rs}(t+\tau) \right\}}{\tau} \le \frac{1}{T} \lambda TF = \lambda F$$
 (61)

where λ is a small positive number and F is the fleet size. τ on the right-hand side of Eq. (61) can be minimized as 1. $\sum_{\tau=1}^{T} \sum_{(r,s)\in\mathscr{Z}^2} \min\left\{w^{rs}(t+\tau), \sum_{i\in\mathscr{A}} y_{ri}^{rs}(t+\tau)\right\}$ is the number of passenger-carrying trips over the (lookahead) time horizon [t,t+T]. It is bounded by the number of parked vehicles at time t, which is bounded by TF. Similarly,

$$\frac{1}{T} \sum_{\tau=1}^{T} \sum_{(r,s) \in \mathscr{Z}^2} \lambda \sum_{i \in \mathscr{A}} y_{ri}^{rs}(t+\tau) \le \frac{1}{T} \lambda TF = \lambda F \tag{62}$$

Therefore Eq. (60) can be rewritten as

$$\frac{1}{T} \sum_{\tau=1}^{T} \sum_{(r,s)\in\mathscr{Z}^{2}} w^{rs}(t) \min \left\{ w^{rs}(t+\tau), \sum_{i\in\mathscr{A}} y^{rs\star}_{ri}(t+\tau) \right\}$$

$$\geq \frac{1}{T} \sum_{\tau=1}^{T} \sum_{(r,s)\in\mathscr{Z}^{2}} w^{rs}(t) \min \left\{ w^{rs}(t+\tau), \sum_{i\in\mathscr{A}} \hat{y}^{rs}_{ri}(t+\tau) \right\} + C \tag{63}$$

where C is the constant generated from Eqs. (61) and (62). Because of Eq. (63), the first term from Eq. (58) satisfies

$$\frac{1}{T} \sum_{\tau=1}^{T} \sum_{(r,s)\in\mathscr{Z}^{2}} 2w^{rs}(t) \left(\bar{d}^{rs} - \min \left\{ w^{rs}(t+\tau), \sum_{i\in\mathscr{A}} y_{ri}^{rs\star}(t+\tau) \right\} \right) \\
\leq \frac{1}{T} \sum_{\tau=1}^{T} \sum_{(r,s)\in\mathscr{Z}^{2}} 2w^{rs}(t) \left(\bar{d}^{rs} - \min \left\{ w^{rs}(t+\tau), \sum_{i\in\mathscr{A}} \hat{y}_{ri}^{rs}(t+\tau) \right\} \right) + C \tag{64}$$

By adding terms $-\sum_{i\in\mathscr{A}}y_{ri}^{rs\star}(t+\tau)+\sum_{i\in\mathscr{A}}y_{ri}^{rs\star}(t+\tau)$ on the left-hand side and terms $-\sum_{i\in\mathscr{A}}\hat{y}_{ri}^{rs}(t+\tau)+\sum_{i\in\mathscr{A}}\hat{y}_{ri}^{rs}(t+\tau)$ on the right-hand side, we can rewrite Eq. (64) as

$$\frac{1}{T} \sum_{\tau=1}^{T} \sum_{(r,s) \in \mathcal{Z}^{2}} 2w^{rs}(t) \left(\bar{d}^{rs} - \sum_{i \in \mathcal{A}} y_{ri}^{rs\star}(t+\tau) + \sum_{i \in \mathcal{A}} y_{ri}^{rs\star}(t+\tau) - \min \left\{ w^{rs}(t+\tau), \sum_{i \in \mathcal{A}} y_{ri}^{rs\star}(t+\tau) \right\} \right) \\
\leq \frac{1}{T} \sum_{\tau=1}^{T} \sum_{(r,s) \in \mathcal{Z}^{2}} 2w^{rs}(t) \left(\bar{d}^{rs} - \sum_{i \in \mathcal{A}} \hat{y}_{ri}^{rs}(t+\tau) + \sum_{i \in \mathcal{A}} \hat{y}_{ri}^{rs}(t+\tau) - \min \left\{ w^{rs}(t+\tau), \sum_{i \in \mathcal{A}} \hat{y}_{ri}^{rs}(t+\tau) \right\} \right) + C \tag{65}$$

Notice that the added terms are bounded by a constant because if $w^{rs}(t+\tau) \geq \sum_{i \in \mathscr{A}} y^{rs}_{ri}(t+\tau)$ then $\sum_{i \in \mathscr{A}} y^{rs}_{ri}(t+\tau) - \min\left\{w^{rs}(t+\tau), \sum_{i \in \mathscr{A}} y^{rs}_{ri}(t+\tau)\right\} = 0$. On the other hand, if $w^{rs}(t+\tau) \leq \sum_{i \in \mathscr{A}} y^{rs}_{ri}(t+\tau)$, $w^{rs}(t)$ can be upper bounded by $\sum_{i \in \mathscr{A}} y^{rs}_{ri}(t+\tau) - \min\left\{w^{rs}(t+\tau), \sum_{i \in \mathscr{A}} y^{rs}_{ri}(t+\tau)\right\}$ can be upper bounded by $\sum_{i \in \mathscr{A}} y^{rs}_{ri}(t+\tau)$. $\sum_{i \in \mathscr{A}} y^{rs}_{ri}(t+\tau)$ is upper bounded by the fleet size F, which yields

$$\frac{1}{T} \sum_{\tau=1}^{T} \sum_{(r,s)\in\mathscr{Z}^{2}} 2w^{rs}(t) \left(\sum_{i\in\mathscr{A}} y_{ri}^{rs}(t+\tau) - \min\left\{ w^{rs}(t+\tau), \sum_{i\in\mathscr{A}} y_{ri}^{rs}(t+\tau) \right\} \right)
\leq 2 \frac{1}{T} T \left(\sum_{i\in\mathscr{A}} y_{ri}^{rs}(t+\tau) \right) \left(\sum_{i\in\mathscr{A}} y_{ri}^{rs}(t+\tau) \right) \leq 2F^{2}$$
(66)

Then Eq. (65) can be rewritten as

$$\frac{1}{T} \sum_{\tau=1}^{T} \sum_{(r,s) \in \mathcal{Z}^2} w^{rs}(t) \left(\bar{d}^{rs} - \sum_{i \in \mathcal{A}} y_{ri}^{rs\star}(t+\tau) \right) \le \frac{1}{T} \sum_{\tau=1}^{T} \sum_{(r,s) \in \mathcal{Z}^2} w^{rs}(t) \left(\bar{d}^{rs} - \sum_{i \in \mathcal{A}} \hat{y}_{ri}^{rs}(t+\tau) \right) + C \tag{67}$$

Since $\hat{\vec{y}}(t+\tau)$ is a sequence with limit $\bar{\vec{y}}$, for every $\eta > 0$ there exists an $M < \infty$ such that for all T > M, $\frac{1}{T} \sum_{\tau=1}^{T} \hat{\vec{y}}(t+\tau) \le |\bar{\vec{y}} - \eta \vec{1}|$ (where $\vec{1}$ is the vector of 1's). Therefore

$$\frac{1}{T} \sum_{\tau=1}^{T} \sum_{(r,s) \in \mathcal{Z}^2} w^{rs}(t) \left(\bar{d}^{rs} - \sum_{i \in \mathcal{A}} \hat{y}^{rs}_{ri}(t+\tau) \right) \leq \sum_{(r,s) \in \mathcal{Z}^2} w^{rs}(t) \left(\bar{d}^{rs} - \sum_{i \in \mathcal{A}} \bar{y}^{rs}_{ri} + \eta \right) + C_1$$

$$(68)$$

where C_1 is a constant. From Lemmas 2 and 3, we know that implementing the dispatch policy with $\bar{y}(t)$ yields

$$\frac{1}{T} \sum_{\tau=1}^{T} \mathbb{E} \left[\sum_{(r,s) \in \mathcal{Z}^2} (w^{rs}(t+\tau+1))^2 - (w^{rs}(t))^2 \middle| \vec{w}(t) \right] \le \kappa_2 - \epsilon |\vec{w}(t)|$$
 (69)

We can choose a M large enough that $\eta - \epsilon \le -\epsilon_2$ for some $\epsilon_2 > 0$. Then

$$\frac{1}{T} \sum_{\tau=1}^{T} \sum_{(r,s)\in\mathscr{Z}^{2}} w^{rs}(t) \left(d^{rs} - \sum_{i\in\mathscr{A}} y^{rs\star}_{ri}(t+\tau) \right) \leq \frac{1}{T} \sum_{\tau=1}^{T} \sum_{(r,s)\in\mathscr{Z}^{2}} w^{rs}(t) \left(d^{rs} - \sum_{i\in\mathscr{A}} \hat{y}^{rs}_{ri}(t+\tau) \right) + C$$

$$\leq \sum_{(r,s)\in\mathscr{Z}^{2}} w^{rs}(t) \left(d^{rs} - \sum_{i\in\mathscr{A}} \bar{y}^{rs}_{ri} + \eta \right) + C + C_{1} \leq -\epsilon_{2} |\vec{w}(t)| + C + C_{1} \tag{70}$$

Using Lemma 4, the main stability result is achieved:

Proposition 4. If $\bar{d} \in \mathcal{D}^0$, then the max-pressure dispatch policy is stabilizing.

Proof. By Lemma 4.

$$\frac{1}{T} \sum_{\tau=1}^{T} \mathbb{E} \left[\sum_{(r,s) \in \mathcal{Z}^2} (w^{rs}(t+\tau+1))^2 - (w^{rs}(t+\tau))^2 \middle| \vec{w}(t) \right] \le \kappa - \epsilon |\vec{w}(t)|$$
 (71)

Taking the sum over T_2 on both sides,

$$\frac{1}{T_2} \sum_{t=1}^{T_2} \mathbb{E} \left[\frac{1}{T} \sum_{\tau=1}^{T} \sum_{(r,s) \in \mathcal{Z}^2} (w^{rs}(t+\tau+1))^2 - (w^{rs}(t+\tau))^2 \right] \leq \frac{1}{T_2} \sum_{t=1}^{T_2} (\kappa - \epsilon |\vec{w}(t)|)$$

Simplifying

$$\frac{1}{T_2} \mathbb{E} \left[\frac{1}{T} \sum_{\tau=1}^{T} \sum_{(r,s) \in \mathcal{Z}^2} (w^{rs} (T_2 + \tau + 1))^2 - (w^{rs} (\tau))^2 \right] \le \frac{1}{T_2} \sum_{t=1}^{T_2} (\kappa - \epsilon |\vec{w}(t)|)$$
(72)

$$\frac{\epsilon}{T_2} \sum_{t=1}^{T_2} |\vec{w}(t)| + \frac{1}{T_2} \mathbb{E} \left[\frac{1}{T} \sum_{\tau=1}^{T} \sum_{(r,s) \in \mathscr{A}^2} (w^{rs} (T_2 + \tau + 1))^2 - (w^{rs} (\tau))^2 \right] \le \kappa$$
 (73)

Taking the limit as $T_2 \to \infty$

$$\lim_{T_2 \to \infty} \left(\frac{\epsilon}{T_2} \sum_{t=1}^{T_2} |\vec{x}(t)| + \frac{1}{T_2} \mathbb{E} \left[\frac{1}{T} \sum_{\tau=1}^{T} \sum_{(r,s) \in \mathscr{A}^2} (w^{rs} (T_2 + \tau + 1))^2 - (w^{rs} (\tau))^2 \right] \right) \le \kappa$$
 (74)

Simplifying.

$$\lim_{T_2 \to \infty} \frac{\epsilon}{T_2} \sum_{t=1}^{T_2} |\vec{w}(t)| \le \kappa \tag{75}$$

which results in $\lim_{T_2 \to \infty} \frac{1}{T_2} \sum_{t=1}^{T_2} |\vec{w}(t)| \le \frac{\kappa}{\epsilon} \quad \Box$

Given bounded queues, we can immediately observe that the average waiting times will also be bounded. This occurs due to Little's Law (Little, 1961), which states that the long-term average number of passengers (denoted by \bar{w}_{rs}) in a stationary system is equal to the long-term average arrival rate (\bar{d}^{rs}) multiplied by the average waiting time (denoted by $\bar{\theta}^{rs}$):

$$\bar{w}^{rs} = \bar{d}^{rs}\bar{\theta}^{rs} \tag{76}$$

Little's Law holds regardless of the distribution of the arrivals and departures.

Corollary 1. When the max-pressure dispatch policy is implemented for $\tilde{d} \in \mathcal{D}^0$, the average waiting time at every zone is also bounded.

Proof. \bar{w}^{rs} is bounded by Proposition 4. By Little's Law, when $\bar{d}^{rs} > 0$ and \bar{w}^{rs} is bounded, $\bar{\theta}^{rs}$ must be bounded also. \Box

5. Simulation model and numerical results

The Sioux Falls network is used to provide a test-case demonstrating the performance of the proposed max-pressure dispatch policy. In contrast to agent-based simulations that seek to characterize the performance of heuristic dispatch policies, the primary purpose of these results is to numerically demonstrate the analytical stability properties discussed above. The network includes 24 nodes and 76 links. It has a total demand of around 10,115 travelers per hour. An agent-based simulation is built in Java, and the optimization program is solved in IBM CPLEX. Since the stability could only be seen after a vehicle redistributing process, we set the simulation duration as 40,000s to ensure it is long enough to demonstrate the stability.

As we mentioned in Section 4.3, the replacement ratio also depends on the demand pattern. Thus, two types of demand patterns are generated and tested in this paper. The default demand pattern in the Sioux Falls network data is tested as the off-peak hour transportation demand, denoted as demand pattern 1. This demand pattern is symmetric, i.e., $\bar{d}^{rS} = \bar{d}^{ST}$. We extend these demand rates to the entire simulation duration with uniformly distributed departure times. However, testing the performance of the proposed policy under asymmetric demand patterns is also important. Thus, a corresponding asymmetric peak-hour demand pattern (denoted demand pattern 2) is also created by setting the nodes marked in orange in Fig. 2 as the only origins. In the default demand file, demand rates between node 10 and node 16 are the highest. Thus, we simulate a scenario in which the area around node 10 and node 16 is the central business district in a city. During the peak hour, all trips originate from this area, and their destination can be any other node. Their departure times distribute uniformly. The simulation is run on a desktop with an Intel Core i5-9400 processor clocked at 2.90 GHz with 24GB of memory.

For the results, three measurements are taken into consideration:

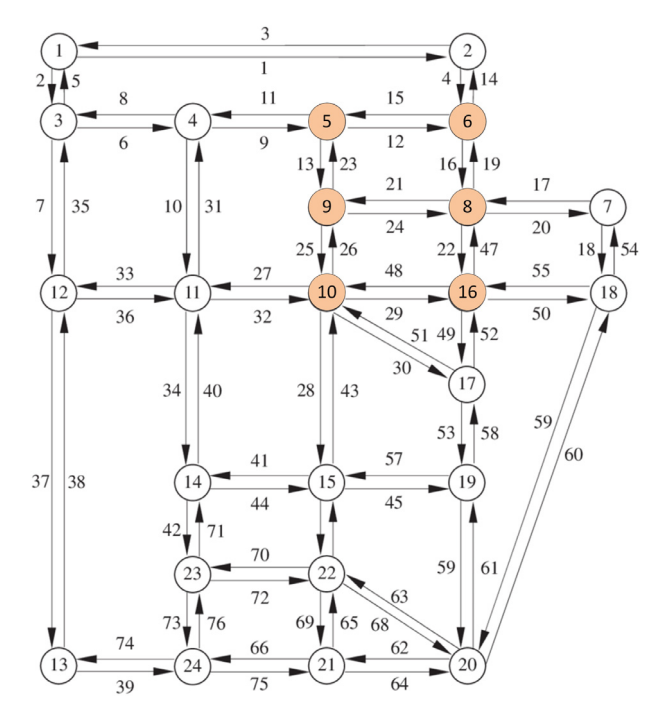


Fig. 2. Sioux Falls network. Nodes in orange denote the central business district used for the asymmetric demand pattern.

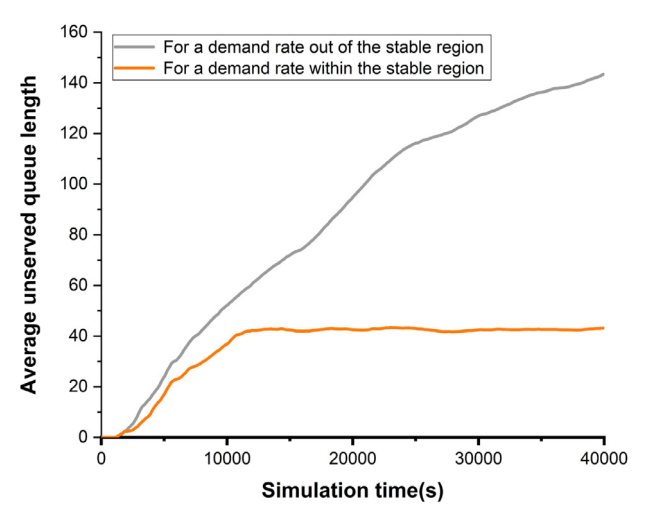


Fig. 3. Difference of queue length for demand rates inside or outside the stable region.

- Average unserved queue length: unserved queue length is defined as the waiting passengers that have no assigned empty vehicle to pick them up right away, nor a vehicle on reallocation trip to pick them up later on. This number is summed over all nodes and averaged by the simulation time.
- Average waiting time: calculated by summing up all served passengers' waiting time (real departure time minus ideal departure time), and averaged over time and the number of passengers served.
- Total number of rebalancing flow happened through the whole analysis period.

First, we show the numerical difference in unserved queue length between the demand inside and outside the stable region. The results are shown in Fig. 3. Clearly, as the simulation goes on, for stable demand, average unserved queue length will fluctuate around a constant number, while for unstable demand, it will continue to increase.

According to the analytical results, a small planning horizon results in inadequate time to plan relocation trips, while a long planning horizon incurs long computation time. In addition, Proposition 3 shows that as the planning horizon increases, the maximum demand that can be served becomes closer to the stable region boundary. Using the simulation tool, we tested the effect of the planning horizon with a demand rate within the stable region. To ensure a sufficiently long time period

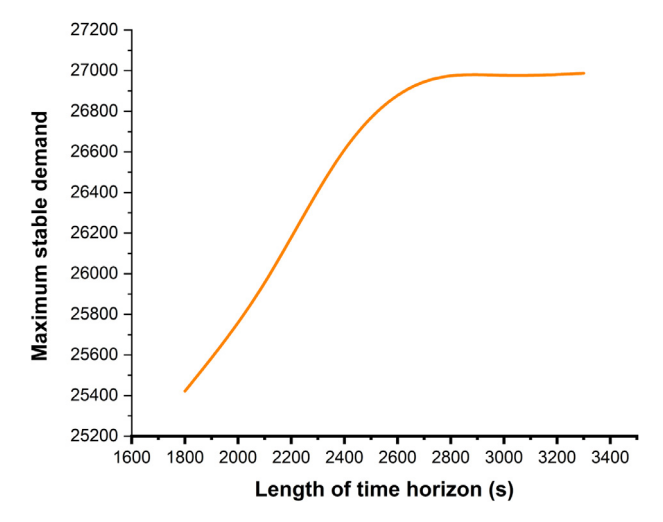


Fig. 4. Maximum stable demand versus length of time horizon.

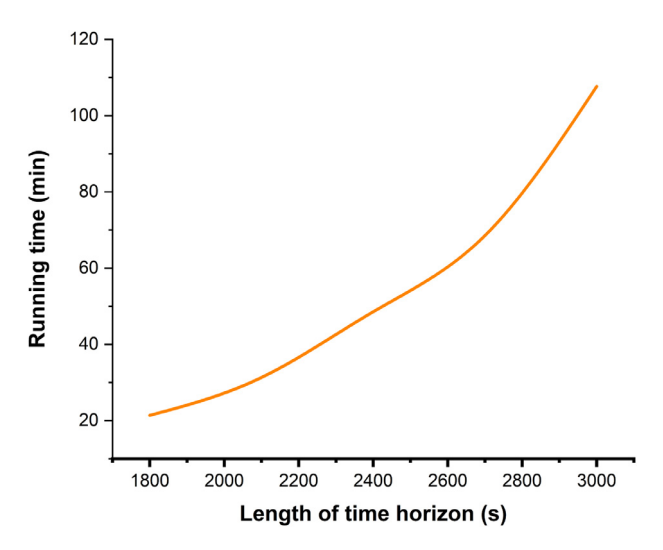


Fig. 5. Running time versus length of time horizon.

to plan relocating trips, the minimum time horizon we considered is 1800 s, since the maximum travel time between two nodes in the network is 1750 s. The fleet size is set to 450. As expected, Fig. 4 shows diminishing returns in the maximum stable demand as the planning horizon increases. When the time horizon is greater than 2700 s, there is no observable improvement in the maximum stable demand. Fig. 5 depicts that the running time increases exponentially as the length of time horizon increases using the maximum stable demand.

We also numerically find the maximum stable demand as the fleet size goes from 200 to 500 vehicles using demand pattern 1 and demand pattern 2. To ensure a large enough planning horizon while maintaining a reasonable running time, we selected a fixed planning horizon of 2400 s for a simulation duration of 40,000 s. As shown in Fig. 6, the relationship between the maximum stable demand and fleet size are roughly linear as expected in analytical results. Off-peak hour demand (pattern 1) has a higher maximum stable demand than peak hour demand (pattern 2). The lack of precise linearity is due to the difficulty in numerically detecting whether a given demand rate is stable.

The average waiting times per person under the maximum stable demand are shown in Fig. 8. Although both average waiting times are captured under the maximum stable demand, the waiting time for pattern 2 is roughly 6 min higher than pattern 1, and the average waiting times for both demand patterns are bounded constants. Pattern 2 has a higher waiting time and rebalancing trips because the asymmetric demand requires significant empty rebalancing, which is depicted in Fig. 7. For the symmetric demand (demand pattern 1), the number of empty rebalancing trips is much lower. Stability would be possible with zero empty rebalancing trips, but some rebalancing occurs due to stochastic variations in demand. For demand pattern 2, the number of rebalancing trips increases linearly with the demand. When rebalancing, the efficiency of a limited fleet resource is impaired, which also explains the higher waiting time for demand pattern 2.

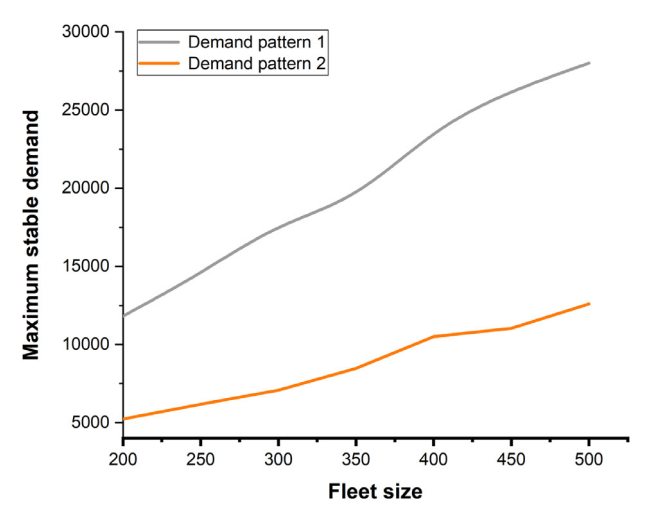


Fig. 6. Maximum stable demand versus given fleet size.

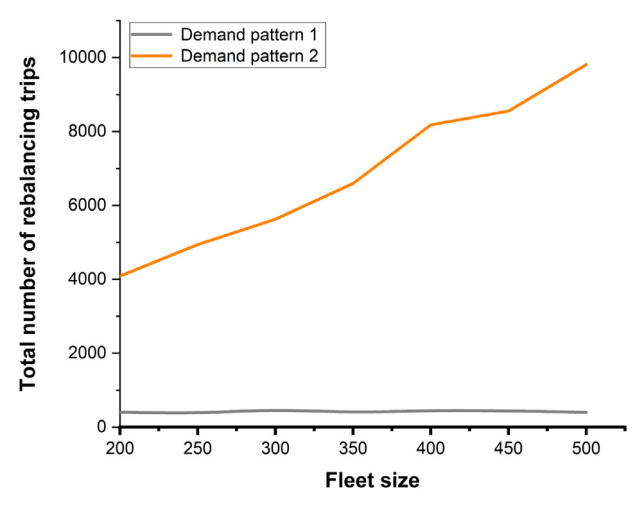


Fig. 7. Total number of rebalancing trips under different demand patterns.

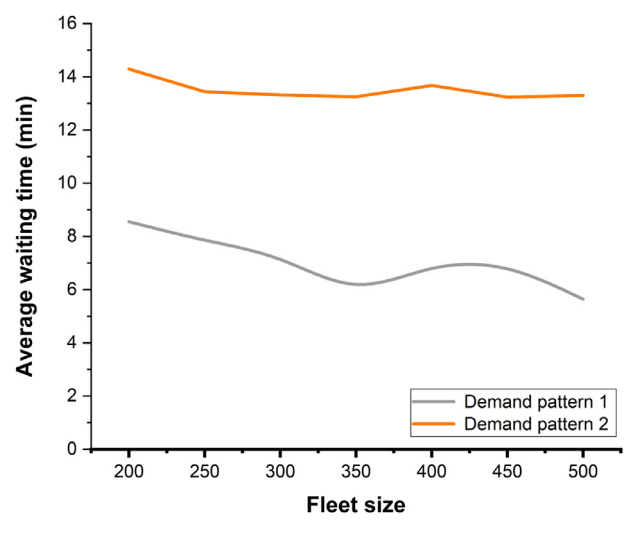


Fig. 8. Average Waiting time per person.

6. Conclusions

This paper analytically establishes a maximum stability dispatch strategy for SAVs. To achieve this, we defined a Markov chain model of SAVs and waiting travelers. We analytically characterize the stable region, or the set of demands that could be served by any dispatch policy. This results in analytical methods of identifying the replacement ratio and minimum fleet size for any given demand patterns. Analytical and numerical results show that the maximum stable demand is linearly related to the fleet size given. Using Lyapunov drift techniques, we prove that the proposed max-pressure dispatch policy will stabilize the network whenever demand is in the stable region. In other words, the max-pressure dispatch policy can serve as much demand as any other dispatch policy. A simulation model is created to test the performance of the proposed max-pressure dispatch policy under symmetric and asymmetric demand patterns. Because it requires more rebalancing trips, the maximum stabilizable demand using the asymmetric demand pattern is less than that of the symmetric demand pattern. The average waiting time is also higher for asymmetric than symmetric demand. After a sufficiently large planning horizon was reached, increasing the planning horizon provided no significant differences in the maximum stabilizable demand.

There are many extensions of SAVs that could be considered in future work, including electric vehicle charging constraints and ridesharing, which may affect the stable region for a given fleet size. One possible way to incorporate ridesharing is to change the objective function which is derived from the max-pressure stability proof, as well as adding constraints for vehicle capacity and complex trajectories. Including congestion and route choice impacts is another crucial point to consider for the future. The proposed dispatch policy could also be studied for more realistic passenger behaviors in agent-based simulations. For instance, the analytical service rate could be studied under the realistic passenger behavior of exiting the system if the waiting times are too long. Overall, there are both analytical and numerical open questions to be addressed in future work.

CRediT authorship contribution statement

Di Kang: Conceptualization, Methodology, Software, Formal analysis, Data curation, Writing - original draft, Writing - review & editing, Visualization. **Michael W. Levin:** Conceptualization, Funding acquisition, Writing - review & editing, Supervision.

Acknowledgments

The authors gratefully acknowledge the support of the National Science Foundation, Award no. 1935514.

References

Alonso-Mora, J., Samaranayake, S., Wallar, A., Frazzoli, E., Rus, D., 2017. On-demand high-capacity ride-sharing via dynamic trip-vehicle assignment. Proc. Natl. Acad. Sci. 114 (3), 462–467.

Banerjee, S., Freund, D., Lykouris, T., 2016. Pricing and optimization in shared vehicle systems: an approximation framework. arXiv preprint arXiv:1608.06819 Bischoff, J., Maciejewski, M., 2016. Simulation of city-wide replacement of private cars with autonomous taxis in berlin. Procedia Comput. Sci. 83, 237–244. Brayerman, A., Dai, J.G., Liu, X., Ying, L., 2019. Empty-car routing in ridesharing systems. Oper. Res. 67 (5), 1437–1452.

Burns, L.D., Iordan, W.C., Scarborough, B.A., 2013. Transforming personal mobility. Earth Inst. 431, 432.

Chen, T.D., Kockelman, K.M., 2016. Management of a shared autonomous electric vehicle fleet: implications of pricing schemes. Transp. Res. Rec. 2572 (1), 37–46.

Chen, T.D., Kockelman, K.M., Hanna, J.P., 2016. Operations of a shared, autonomous, electric vehicle fleet: implications of vehicle & charging infrastructure decisions. Transp. Res. Part A 94, 243–254.

Fagnant, D.J., Kockelman, K., 2015. Preparing a nation for autonomous vehicles: opportunities, barriers and policy recommendations. Transp. Res. Part A 77, 167–181.

Fagnant, D.J., Kockelman, K.M., 2014. The travel and environmental implications of shared autonomous vehicles, using agent-based model scenarios. Transp. Res. Part C 40, 1–13.

Fagnant, D.J., Kockelman, K.M., 2018. Dynamic ride-sharing and fleet sizing for a system of shared autonomous vehicles in austin, texas. Transportation 45 (1), 143–158.

(1), 143-138. Fagnant, D.J., Kockelman, K.M., Bansal, P., 2015. Operations of shared autonomous vehicle fleet for Austin, Texas market. Transp. Res. Rec. 2536, 98-106. lacobucci, R., McLellan, B., Tezuka, T., 2018. Modeling shared autonomous electric vehicles: potential for transport and power grid integration. Energy 158,

148–163.

Kanoria, Y., Qian, P., 2019. Near optimal control of a ride-hailing platform via mirror backpressure. arXiv–1903.

Leonardi, E., Mellia, M., Neri, F., Marsan, M.A., 2001. Bounds on average delays and queue size averages and variances in input-queued cell-based switches. In: INFOCOM 2001. Twentieth Annual Joint Conference of the IEEE Computer and Communications Societies. Proceedings. IEEE, 2. IEEE, pp. 1095–1103. Levin, M.W., 2017. Congestion-aware system optimal route choice for shared autonomous vehicles. Transp. Res. Part C 82, 229–247.

Levin, M.W., Kockelman, K.M., Boyles, S.D., Li, T., 2017. A general framework for modeling shared autonomous vehicles with dynamic network-loading and dynamic ride-sharing application. Comput. Environ. Urban Syst. 64, 373–383.

Levin, M.W., Odell, M., Samarasena, S., Schwartz, A., 2019. A linear program for optimal integration of shared autonomous vehicles with public transit. Transp. Res. Part C 109, 267–288.

Little, J.D., 1961. A proof for the queuing formula: $L = \lambda$ w. Oper. Res. 9 (3), 383–387.

Ma, H., Fang, F., Parkes, D. C., 2018. Spatio-temporal pricing for ridesharing platforms. arXiv preprint arXiv:1801.04015

Ma, J., Li, X., Zhou, F., Hao, W., 2017. Designing optimal autonomous vehicle sharing and reservation systems: a linear programming approach. Transp. Res. Part C 84, 124–141.

Maciejewski, M., Bischoff, J., 2016. Congestion effects of autonomous taxi fleets. Transport 33 (4), 971-980.

Martinez, L., Crist, P., 2015. Urban mobility system upgrade-how shared self-driving cars could change city traffic. International Transport Forum, Paris.

Moorthy, A., De Kleine, R., Keoleian, G., Good, J., Lewis, G., 2017. Shared autonomous vehicles as a sustainable solution to the last mile problem: a case study of ann arbor-detroit area. SAE Int. J. Passeng.Cars-Electronic Electr. Syst. 10 (2017-01–1276), 328–336.

Ohnemus, M., Perl, A., 2016. Shared autonomous vehicles: catalyst of new mobility for the last mile? Built Environ. 42 (4), 589-602.

Pavone, M., Smith, S.L., Frazzoli, E., Rus, D., 2012. Robotic load balancing for mobility-on-demand systems. Int. J. Robot. Res. 31 (7), 839-854.

Scheltes, A., de Almeida Correia, G.H., 2017. Exploring the use of automated vehicles as last mile connection of train trips through an agent-based simulation model: an application to delft, netherlands. Int. J. Transp. Sci. Technol. 6 (1), 28-41.

Shen, Y., Zhang, H., Zhao, J., 2018. Integrating shared autonomous vehicle in public transportation system: a supply-side simulation of the first-mile service in singapore. Transp. Res. Part A 113, 125-136.

Spieser, K., Treleaven, K., Zhang, R., Frazzoli, E., Morton, D., Pavone, M., 2014. Toward a systematic approach to the design and evaluation of automated mobility-on-demand systems: a case study in singapore. In: Road Vehicle Automation. Springer, pp. 229–245. Varaiya, P., 2013. Max pressure control of a network of signalized intersections. Transp. Res. Part C 36, 177–195.

Volkov, M., Aslam, J., Rus, D., 2012. Markov-based redistribution policy model for future urban mobility networks. In: 2012 15th International IEEE Conference on Intelligent Transportation Systems. IEEE, pp. 1906–1911.

Zhang, R., Pavone, M., 2016. Control of robotic mobility-on-demand systems: a queueing-theoretical perspective. Int. J. Robot. Res. 35 (1–3), 186–203. Zhang, R., Rossi, F., Pavone, M., 2016. Model predictive control of autonomous mobility-on-demand systems. In: 2016 IEEE International Conference on Robotics and Automation (ICRA). IEEE, pp. 1382-1389.

Zhang, R., Rossi, F., Pavone, M., 2016b. Routing autonomous vehicles in congested transportation networks: structural properties and coordination algorithms. arXiv preprint arXiv:1603.00939